Author's personal copy

Applied Surface Science 255 (2008) 2133–2138

Contents lists available at ScienceDirect

Applied Surface Science

journal homepage: www.elsevier.com/locate/apsusc

Effect of substrate temperature on the structural properties of magnetron sputtered titanium nitride thin films with brush plated nickel interlayer on mild steel

B. Subramanian *, K. Ashok, M. Jayachandran

ECMS Division, Central Electrochemical Research Institute, Karaikudi 630006, India

ARTICLE INFO

Article history:
Received 26 December 2007
Received in revised form 21 March 2008
Accepted 2 July 2008
Available online 19 July 2008

PACS:
81.15. Cd
68.55. Jk

Keywords:
Titanium nitride
Magnetron sputtering
Structural properties
Hard coatings

ABSTRACT

Thin films of titanium nitride (TiN) were prepared on mild steel (MS) by a physical vapor deposition (PVD) method namely direct current reactive magnetron sputtering. With the aim of improving the adhesion of TiN layer an additional Nickel interlayer was brush plated on the steel substrates prior to TiN film formation. The phase has been identified with X-ray diffraction (XRD) analysis, and the results show that the prominent peaks observed in the diffraction patterns correspond to the (1 1 1), (2 0 0) and (2 2 2) planes of TiN. Cross-sectional SEM indicated the presence of dense columnar structure. The mechanical properties (modulus and hardness) of these films were characterized by nanoindentation.

© 2008 Elsevier B.V. All rights reserved.

1. Introduction

In recent years, usage of thin, hard and wear resistant titanium nitride (TiN) ceramic coatings in metal cutting and metal forming tools applications has acquired increasing importance. It plays a vital role in many industrial applications because of its high hardness, high evaporation temperature (2950 °C), good chemical stability and metallic brightness [1]. Generally, techniques like physical vapor deposition (PVD) [2,3], plasma assisted chemical vapor deposition (PACVD), plasma enhanced chemical vapor deposition (PECVD) and hollow cathodic ionic plating [4] are used in developing hard coatings on various substrates.

The equilibrium phase diagram of TiN shows three stable solid phases. The cubic B1-NaCl crystal structure of δ-TiN phase is stable over a wide composition range ($0.6 < N/Ti < 1.2$) and the hexagonal α-Ti phase can dissolve up to 15 at.% nitrogen. The ε-Ti_2N crystallizes in a tetragonal structure and exists only at a composition range of 33 at.%. However, the δ-TiN phase is mostly used in technological applications [5]. Pelleg et al. [6] have shown that for these types of material, the actual plane of lowest surface energy is the (2 0 0). They also suggested that the (1 1 1) plane in TiN possesses the lowest strain energy, due to anisotropy of Young's modulus, and that this frequently observed orientation is due to a minimization of strain energy. The structure and the properties of films depend sensitively on the deposition conditions. The TiN coatings produced by PVD route like sputtering method have better materials properties and thermal stability [7]. The dependence of the structural and other physiochemical properties of TiN layers deposited by DC magnetron sputtering on the substrate bias voltage and substrate position was investigated. The formation of TiN compound depends mainly on neutral atomic and excited molecular nitrogen species arising within the magnetron discharge [8].

The aim of the present work is to study the effect of substrate temperature on structure of TiN thin film and with brush plated Ni interlayer on mild steel (MS) substrate deposited by reactive DC magnetron sputtering. The structural parameters, viz. the crystallinity, crystal phase, lattice constant, grain size, orientation,

* Corresponding author. Tel.: +91 4565 227555; fax: +91 4565 227713.
E-mail address: tspsenthil@yahoo.com (B. Subramanian).

0169-4332/$ – see front matter © 2008 Elsevier B.V. All rights reserved.
doi:10.1016/j.apsusc.2008.07.083

Author's personal copy

internal stress and strain are strongly dependent on the substrate temperature. Scanning electron microscopy was applied for precise investigation of surface topography of nitride layers. Such information is essential for understanding the interaction of the outer surface of these layers with a biological environment [9].

2. Experimental

The used substrate was MS, consisting of 0.37 wt% C, 0.28 wt% Si, 0.66 wt% Mn and 98.69 wt% Fe. Coupons of the substrate were cut to size of 75 mm × 25 mm and the surface was ground with SiC paper to remove the oxides and other contamination. The polished substrates were degreased with acetone and then cathodically electro cleaned in alkali solution containing sodium hydroxide and sodium carbonate for 2 min at 70 °C, followed by rinsing with triple distilled water. These substrates were subsequently dipped in 5 vol.% H_2SO_4 solution for 1 min and thoroughly rinsed in distilled water.

A microprocessor controlled Selectron Power Pack Model 150 A to 40 V (USA) was used to transform AC current to DC current in the brush plating setup. The schematic of the brush plating system is given elsewhere [10]. The DC power pack has two leads, one is the anode connected to the plating tool and the other is the cathode connected to the work piece over which the coating has to be plated. The anode is covered with a porous absorbant material, which acts as the brush holds the solution. This wet brush can be moved on the surface of the work piece that is to be finished (coated). When the anode touches the work surface the electrical circuit is closed and deposition is produced. The nickel electrolyte bath, similar to Watt's bath, contained 240-g/l nickel sulphate, 40-g/l nickel chloride and 30-g/l boric acid. The pH and temperature was maintained at 4.0 and 28 °C (RT), respectively.

The layers of TiN were deposited on well-cleaned MS substrates and brush plated Ni/MS specimen using a DC magnetron sputtering unit HIND HIVAC. The base pressure of the chamber was below 10^{-6} Torr (1.33×10^{-4} Pa) and the substrate temperature was varied between 200 °C and 500 °C. High purity argon was fed into the vacuum chamber for the plasma generation. The substrates were etched for 5 min at a DC power of 50 W and an argon pressure of 10 mTorr (1.33 Pa). A high purity (>99.999%) Ti target of 7.5 cm diameter was used as cathode.

X-ray diffraction (XRD) was used to examine the changes in preferred grain orientation. XRD patterns were recorded using an X'pert pro diffractometer using Cu Kα (1.541 Å) radiation from 40 kV X-ray source running at 30 mA. The surface of the coating was characterized by scanning electron microscopy (SEM) using a Hitachi S 3000H microscope. The hardness of the TiN thin films was measured using nanoindentation. The loading and unloading phases of indentation were carried out over a time span of approximately 20 s in all the experiments. At the maximum load, a dwell period of 20 s was imposed before unloading, and another dwell period of 20 s at 90% of unloading, so as to correct for any thermal drift in the system. At least 20 indents were made for each specimen, with the adjacent indents separated by at least 10 μm.

3. Results and discussion

3.1. Structural properties

The XRD patterns of DC magnetron sputtered TiN thin films deposited at various substrate temperatures (T_s) are shown in Fig. 1(a)–(d). The *d* spacing values matches with JCPDS card no. 38-1420 for TiN thin film. Only a single-phase TiN structure with FCC and the peaks corresponding to (1 1 1) and (2 0 0) planes are observed at $2\theta = 36.4°$ and 42.2°. The outcome revealed that the

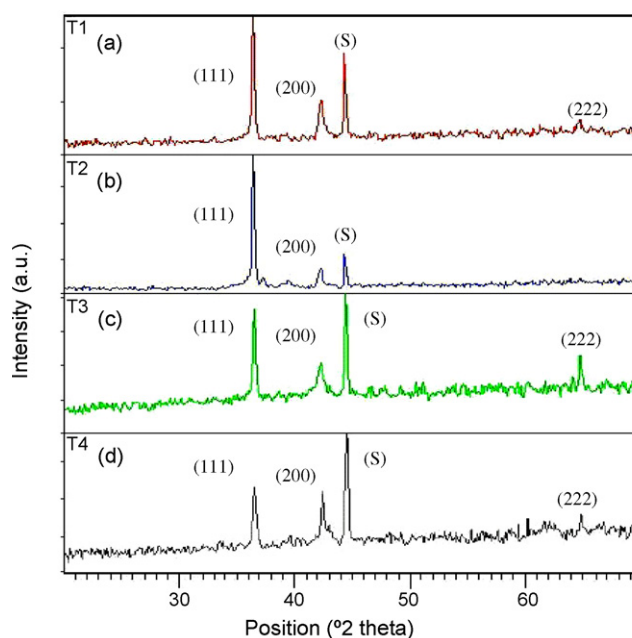

Fig. 1. XRD pattern for TiN at different substrate temperatures: (a) 200 °C, (b) 300 °C, (c) 400 °C and (d) 500 °C.

homogeneous coating displays a strong preferred (1 1 1) orientation parallel to the substrate surface. The (1 1 1) plane of TiN has the lowest strain energy due to anisotropy in Young's modulus as observed from nanoindendation studies also. Therefore, its alignment normal to the growing direction will minimize the total energy under strain–energy dominated growth [5]. When the substrate temperature increased, the peak intensity of (1 1 1) plane was found decreasing whereas the intensity of (2 0 0) plane showed an increasing trend. This means that the crystallographic orientation of the film changes from the presence of (1 1 1) to both (1 1 1) and (2 0 0) with the increase of T_s. Comparatively, one can observe that the sample prepared at $T_s = 400$ °C shows good crystalline nature as observed from (1 1 1) (2 0 0) and (2 2 2) planes. It confirms the textured growth of the film with different planes to improve its strength.

XRD patterns of TiN coatings with Ni interlayer on MS substrates at different substrate temperatures (T_s) are shown in Fig. 2(a)–(d). The patterns show the predominant peaks for FCC Ni (JCPDS card no. 04-0850) interlayer along (1 1 1) and (2 0 0) planes in addition to that peaks identified for TiN along (1 1 1) and (2 0 0) planes at $2\theta = 36.4°$ and 42.3°. A constant thickness of about (∼5 μm) Ni interlayer was maintained for all the samples. Up to 400 °C the peak intensity of TiN (1 1 1) plane increases and the intensity of (2 0 0) was found to increase at 500 °C.

The structural parameters calculated for both (1 1 1) and (2 0 0) planes were compared and both behave close to one another. The lattice parameter of the TiN sample prepared at 200 °C (T_s) was calculated to be 4.27 Å, which is in good agreement with the reported value (JCPDS No. 38-1420) lattice constant vs. substrate temperature graph for both (1 1 1) and (2 0 0) planes are shown in Fig. 3a. When T_s increases the lattice parameter decreases [11] in accordance with the decrease of crystallographic volume. The value of the lattice parameter for the TiN thin film is lower than the reported value for the bulk [12] means that the lattice has many nitrogen vacancies [13]. These vacancies increase with the temperature because the re-sputtering process affects the lighter N atoms more than heavier Ti atoms.

Author's personal copy

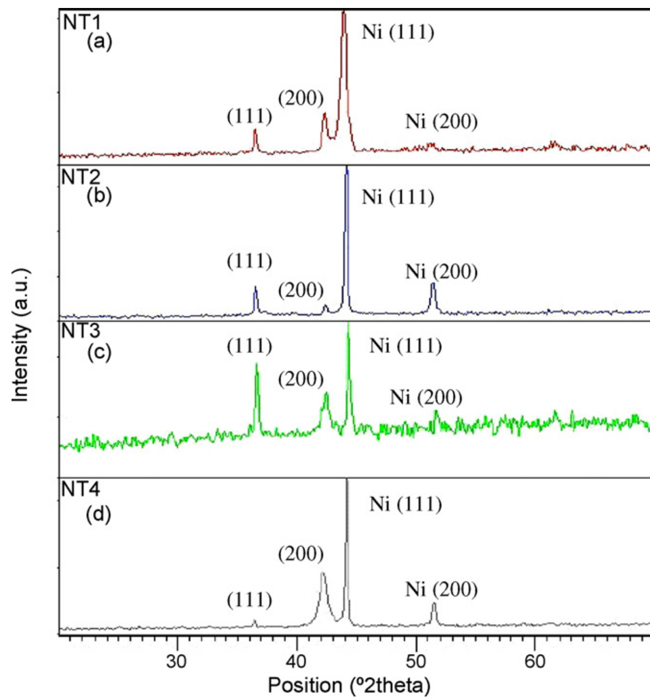

Fig. 2. XRD pattern for TiN with Ni interlayer at different substrate temperatures: (a) 200 °C, (b) 300 °C, (c) 400 °C and (d) 500 °C.

In the case of TiN thin film, with Ni interlayer deposited up to 400 °C, the lattice constant is observed to decrease for both (1 1 1) and (2 0 0) planes as shown in Fig. 3b. An increase in lattice constant is observed beyond 500 °C for the (2 0 0) plane, which may be attributed to the increase in full width half maximum (FWHM) for this particular plane. The change in lattice constant may be due to the film grains that are strained and that may be present owing to the change of nature and concentration of the native imperfections [14].

Using the broadening of the peaks, it is possible to determine the crystallite size, strain and dislocation density from Scherrer formula (Warren) [15]. The grain size (D) of the coatings was determined by the equation:

$$D = \frac{0.94\lambda}{\beta\cos\theta} \quad (1)$$

where β is the FWHM of the diffraction peak, λ is the wavelength of the incident Cu Kα X-ray (1.514 A?), and θ is the diffraction angle. While increasing the T_s, grain size decreased whereas strain and dislocation density were found to increase. The larger grain size of the film grown at 200 °C is also an evidence of its high compaction (decreasing the grain boundaries) confirmed by the highest intensity of the diffraction peak at this temperature. The grain size curve shown in Fig. 4a is highly influenced by the substrate temperature. At very high temperatures, desorption process appears, because the adsorption energy is greater than the surface energy and the ad atoms are desorbed [16] leading to the reduction in grain size.

Whereas for the TiN thin film with Ni interlayer, when the temperature is increased, the mobility of the ad atoms also increases as in Fig. 4b, favoring grouping and nucleation and thereby producing an increase in the grain size. This provides larger area of contact between adjacent crystallite, facilitating coalescence process to form larger crystallites [17]. But there is a limit in this process. It is because at very high temperatures, the ad atoms desorption occurs which results in the deposition of less material on the surface and makes the grain size smaller [18,19].

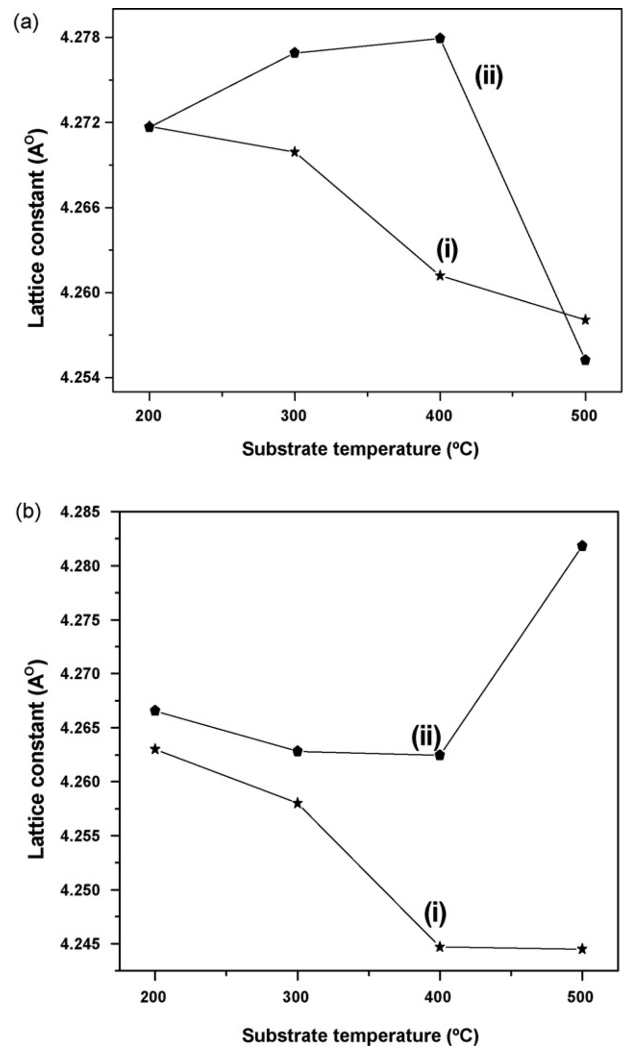

Fig. 3. (a) Variation of the lattice constant with the substrate temperature of (i) 1 1 1 plane and (ii) 2 0 0 plane of TiN thin films; (b) variation of the lattice constant with the substrate temperature of (i) 1 1 1 plane and (ii) 2 0 0 plane of TiN thin films with Ni interlayer.

The micro-strain (ε) was calculated from the relation [15]:

$$\varepsilon = \frac{\beta\cos\theta}{4} \quad (2)$$

The dislocation density (δ) [15], defined as the length of the dislocation per unit volume of the crystal, was calculated from:

$$\delta = \frac{15\varepsilon}{aD} \quad (3)$$

where a is the lattice constant. It is observed that both micro-strain (ε) and dislocation density (δ) increase beyond 300 °C for TiN thin film and TiN/Ni/MS and the values are given in Tables 1 and 2, respectively. The decreasing trend is due to the movement of interstitial atoms from inside the crystallites to its grain boundary, which dissipates leading to the reduction in the concentration of lattice imperfection [14]. The lattice distortions are responsible for reduction in dislocations [20]. Since dislocation density and strain are the manifestation of dislocation network in the films, the

Author's personal copy

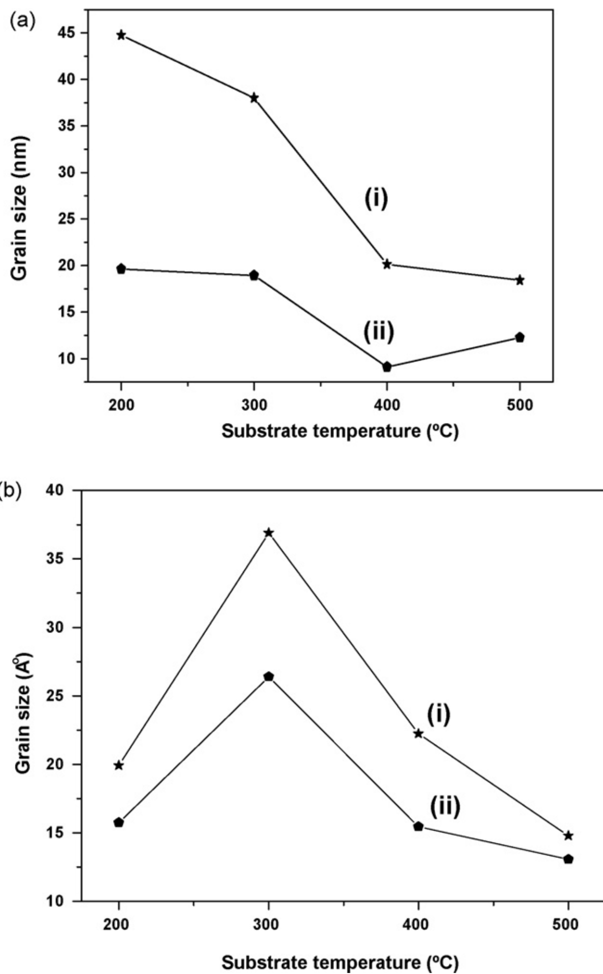

Fig. 4. (a) Variation of grain size with the substrate temperature of (i) 1 1 1 plane and (ii) 2 0 0 plane for TiN thin film; (b) variation of the grain size with the substrate temperature of (i) 1 1 1 plane and (ii) 2 0 0 plane of TiN thin film with Ni interlayer.

Table 1
Structural parameters calculated for TiN thin film

Substrate temperature, T_s (°C)	Plane ($h\,k\,l$)	Stress, σ (GPa)	Strain, ε ($\times 10^{-3}$)	Dislocation density, δ ($\times 10^{-15}$)	Texture coefficient, T_c
200	1 1 1	−8.9	0.795	0.62	1.554
	2 0 0	−8.9	1.812	3.24	0.445
300	1 1 1	−8.4	0.936	8.65	1.806
	2 0 0	−10.4	1.879	3.48	0.193
400	1 1 1	−6.0	1.767	3.09	1.533
	2 0 0	−10.7	3.914	15.12	0.466
500	1 1 1	−5.1	1.931	3.69	1.254
	2 0 0	−4.3	2.906	8.37	0.754

decrease in dislocation density indicates the formation of high-quality films at higher substrate temperatures. This becomes possible due to the fact that when the substrate is kept at higher temperature, the dislocations get more thermal energy and have a higher mobility [21].

The stress values are found to increase for the (1 1 1) plane. Thornton and Hoffmann [22] revealed that vacuum evaporated films are in a state of stress. The total stress is composed of a thermal stress and an intrinsic stress. The thermal stress is due to the difference in the thermal expansion coefficients of the film and substrate material. The intrinsic stress is due to the accumulating

Table 2
Structural parameters calculated for TiN thin film with Ni interlayer

Substrate temperature, T_s (°C)	Plane ($h\,k\,l$)	Stress, σ (GPa)	Strain, ε ($\times 10^{-3}$)	Dislocation density, δ ($\times 10^{-15}$)	Texture coefficient, T_c
200	1 1 1	−6.5	1.785	3.15	0.901
	2 0 0	−7.5	2.276	5.08	1.099
300	1 1 1	−5.1	0.964	0.92	1.581
	2 0 0	−6.4	1.348	1.79	0.417
400	1 1 1	−2.1	1.595	2.53	1.348
	2 0 0	−6.3	2.302	5.24	0.652
500	1 1 1	−1.8	2.345	5.58	0.499
	2 0 0	−11.8	2.653	7.11	1.500

effect of the crystallographic flaws that are built in the film during deposition. It is difficult to avoid thermal stress for film deposited at any temperature.

The average internal stress for the film deposited at high temperature is found to be compressive in nature. The formation of compressive stress can be attributed to native defects arising from the lattice misfit. The defects have a probability to migrate parallel to the film surface with the surface mobility modified by the substrate temperature so that the films have the tendency to expand and develop an internal compressive stress.

The XRD results reveal the fact that when a metal is under stress (applied or residual), the resulting elastic strains can cause the atomic planes in the metallic crystal structure to change their spacing. When a polycrystalline metal is subjected to stress, elastic strains will be produced in the individual crystallite present in the crystal lattice [23].

The internal/residual stresses developed inside the metal matrix due to plastic deformation are tensile in nature. For the (2 0 0) plane stress value decreases which arises due to the phase transformation produced at elevated temperature during the heat treatment steps, since the density of any two phases is not the same and there will be localized changes, either decrease or increase in volume [24].

The value of texture coefficient (T_c) was calculated using the equation:

$$T_c = \frac{I_m(h\,k\,l)/I_0(h\,k\,l)}{(1/n)\sum_1^n I_m(h\,k\,l)/I_0(h\,k\,l)} \tag{4}$$

where $I_m(h\,k\,l)$ is the reflected intensity from $h\,k\,l$ crystallographic planes in the textured specimen and $I_0(h\,k\,l)$ is the standard intensity, and n is the total number of reflections measured. The T_c value for a particular set of $(h\,k\,l)$ planes is proportional to the number of grains that are oriented with this plane parallel to the surface of the specimen. The T_c values of TiN and Ni interlayer TiN thin films calculated for (1 1 1) and (2 0 0) plane show a similar trend as observed from Tables 1 and 2, respectively. The values show the variation of the texture coefficient corresponding to (1 1 1) and (2 0 0) peak with substrate temperature. The strength of (1 1 1) and (2 0 0) orientations was represented by the texture coefficient $\{I(1\,1\,1)/[I(1\,1\,1) + I(2\,0\,0)]\}$ and $\{I(2\,0\,0)/[I(1\,1\,1) + I(2\,0\,0)]\}$, where I is the integrated intensity of the corresponding Bragg peak from a Gaussian fit. The increase in texture coefficient with substrate temperature indicates an improvement in the crystalline nature of the layers [25]. An increase in T_c of (2 0 0) plane was observed beyond the substrate temperature of 300 °C and this may be due to enhancement of the reduction mechanism of the imperfections originating from lattice misfit in the films.

Author's personal copy

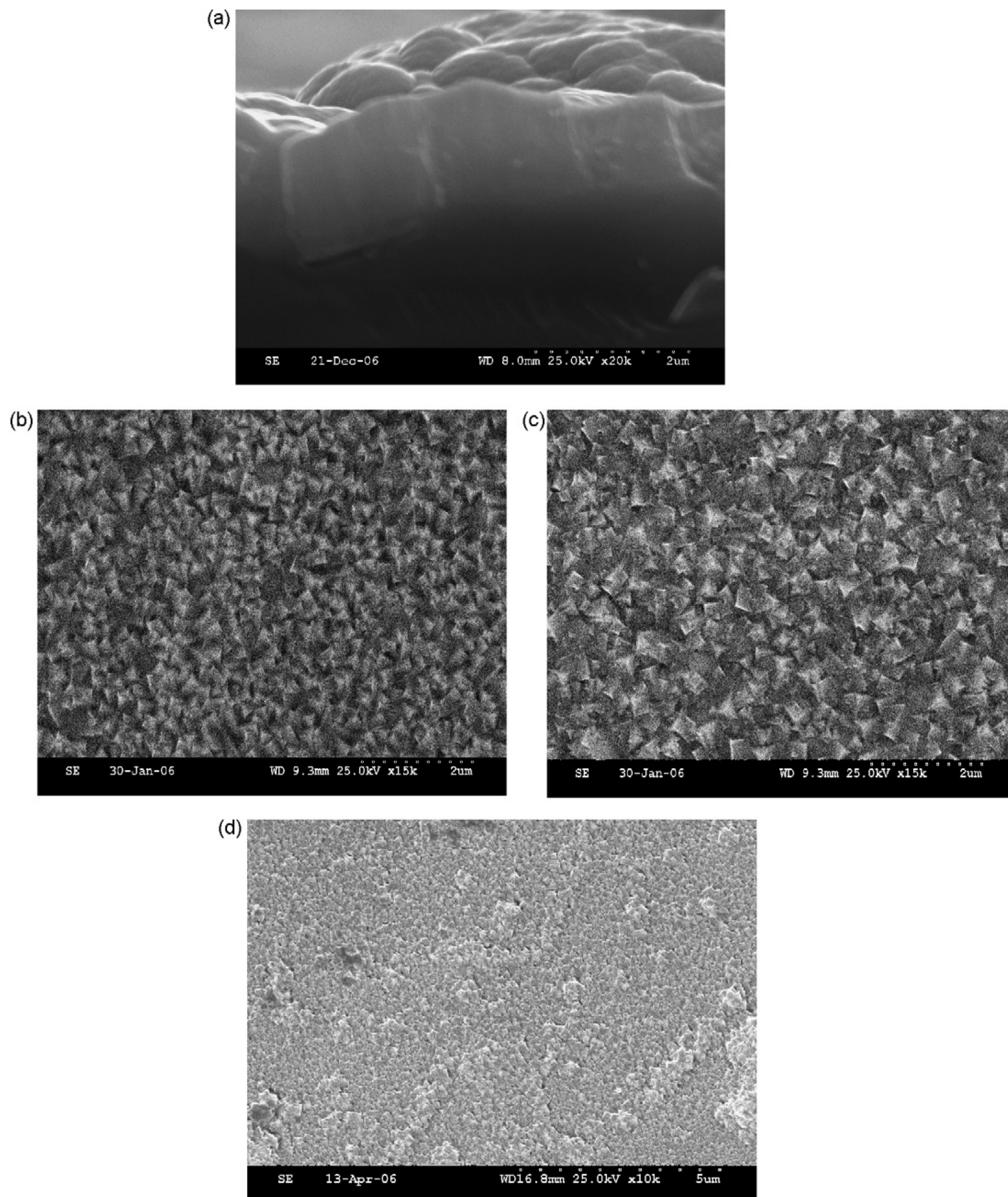

Fig. 5. (a) Cross-sectional view of TiN thin film. Surface morphology of TiN film: (b) TiN film on MS at 400 °C, (c) TiN film with Ni interlayer on MS at 400 °C and (d) TiN film with Ni interlayer on MS at 500 °C.

3.2. Surface morphology

The cross-sectional and plane SEM photographs of TiN film on MS deposited at optimized condition are shown in Fig. 5a and b. It is evident that the TiN films have a columnar structure (Fig. 5a) with voids and boundaries throughout the film thickness. This growth process is similar to that reported in the literature for TiN films [26]. This morphological study is very important for studying the oxidation mechanism of these films since oxygen can diffuse through the voids present in between the columns and grain boundaries. Hones et al. [27] have shown that in the case of the binary TiN system the morphology of the coatings significantly influences the oxidation rate and films with a pronounced columnar morphology oxidize seven times faster than those with a dense- and fine-grained morphology.

The precise nature of the coating microstructure depends on the mobility of deposited ad atoms which in turn can be influenced by the deposition temperature, working gas pressure, interlayer and the deposition parameters such as the substrate bias [28]. In general PVD films deposited without an interlayer show an open columnar structure of zone 1 type according to the structure model of Thornton [29]. Such films have a relatively low hardness and poor wear resistance [30] and do not support any thermal contributions to the overall residual stress, because of the possibility of relaxation of the column boundaries into the intercolumnar spaces perpendicular to the substrate surface. The introduction of a 5 μm thick brush plated Ni interlayer leads to a much more dense and bigger grain size as shown in Fig. 5c.

Author's personal copy

3.3. Nanomechanical properties

Nanoindentation provides a method of near surface measurements to reduce substrate effect because the direct observation of the contact impression size is not necessary. The nanohardness can be evaluated from the following equation [31]:

$$H = \frac{P_{\max}}{A} \quad (5)$$

where $P_{\max}$ is the maximum load and A is the projected area determined from the function of depth. Upon unloading, the elastic displacements were recovered and the plastic displacements were retained. The indentation depth was lower than 100 nm, which in turn was less than 10% of the film thickness used. The nanohardness and the Young's modulus of the TiN thin film on MS and TiN thin film with Ni interlayer on MS prepared at the optimized T_s of 400 °C were 16.6 GPa and 260.7 GPa and 17.3 GPa and 258 GPa, respectively. The higher value of hardness could be because of the presence of strained domains.

4. Conclusions

In the present study, TiN thin films were successfully deposited on MS and with about 5.0 μm thick brush plated Ni interlayer by reactive DC magnetron sputtering technique. These films had preferred orientation along (1 1 1) and (2 0 0). For TiN with Ni interlayer thin film, texture coefficients of (2 0 0) plane are found to increase which shows the improvement in the crystallinity of the layers. TiN films had columnar structure with voids and boundaries and with the Ni interlayer, a denser microstructure was observed.

Acknowledgement

One of the authors (B.S.) thanks the Department of Science & Technology, New Delhi for a research grant under SERC Fast Track Scheme No. SR/FTP/CS-23/2005.

References

[1] J. Bonse, P. Rudolph, J. Kruger, S. Baudach, W. Kautek, Appl. Surf. Sci. 154/155 (2000) 659.
[2] S.V. Hainsworth, W.C. Soh, Surf. Coat. Technol. 163 (2003) 515.
[3] H.D. Na, H.S. Parka, D.H. Junga, G.R. Leea, J.H. Joob, J.J. Leena, Surf. Coat. Technol. 41 (2003) 169.
[4] Li Ying, Li Qu, F. Wang, Corros. Sci. 45 (2003) 1367.
[5] C. Albano, Th. Jeff, M. De Hosson, Nanostructured Coatings, Springer, 2006,, p. 183.
[6] J. Pelleg, L.Z. Zevin, S. Lungo, N. Croitoru, Thin Solid Films 197 (1991) 117.
[7] G. Polykove, T. Hubert, Surf. Coat. Technol. 141 (2001) 55.
[8] F. Richter, H. Kupfer, H. Giegengack, G. Schaarschmidt, F. Scholze, F. Elstner, G. Hecht, Surf. Coat. Technol. 54/55 (1992) 338.
[9] M.-N. Agnieszka, N. Robert, J. Alloys Compd. 424 (2006) 272.
[10] B. Subramanian, S. Mohan, S. Jayakrishnan, M. Jayachandran, Curr. Appl. Phys. 7 (2007) 305.
[11] H. Jimenez, E. Restrepo, A. Devia, Surf. Coat. Technol. 201 (2006) 1594.
[12] M.I. Jones, I.R. McColl, D.M. Grant, Surf. Coat. Technol. 132 (2000) 143.
[13] A.J. Perry, J.P. Schaffer, J. Brunner, W.D. Sproul, Surf. Coat. Technol. 49 (1991) 188.
[14] P.K.R. Kalita, B.K. Sarma, Das, Bull. Mater. Sci. 23 (2000) 313.
[15] B.E. Warren, X-ray Diffraction, Addison Wesley Publishing Co., London, 1969, p. 18.
[16] J.A. Thornton, Annu. Rev. Mater. Sci. 7 (1997) 239.
[17] P.S. Patil, R.K. Kawar, T. Seth, D.P. Amalnerkar, P.S. Chigare, Ceram. Int. 29 (2003) 725.
[18] D.-K. Lee, J.-J. Lee, J. Joo, Surf. Coat. Technol. 174 (2003) 1234.
[19] H. Jiménez, E. Restrepo, A. Devia, Surf. Coat. Technol. 201 (2006) 1594.
[20] F. Vaz, J. Ferreira, E. Ribeiro, L. Rebouta, S. Lanceros-Méndez, J.A. Mendes, E. Alves, Ph. Goudeau, J.P. Rivière, F. Ribeiro, I. Moutinho, K. Pischow, J. de Rijk, Surf. Coat. Technol. 191 (2005) 317.
[21] V. Senthilkumar, S. Venkatachalam, C. Viswanathan, S. Gopal, Sa.K. Narayandass, D. Mangalaraj, K.C. Wilson, K.P. Vijayakumar, Cryst. Res. Technol. 40 (2005) 573.
[22] J.A. Thornton, D.W. Hoffmann, Thin Solid Films 171 (1989) 5.
[23] O.R. Clayton, "Residual Stress Measurements" ASM Handbook—Mechanical Testing and Evaluation, vol. 8, ASM International, Ohio, 2000, pp. 898–899.
[24] M. Meier, Thesis, Department of Chemical Engineering & Material Science, University of California, Davis, 2004.
[25] K.T. Ramakrishna Reddy, G.M. Shanthini, D. Johnston, R.W. Miles, Thin Solid Films 427 (2003) 397.
[26] J.W. Lim, H.S. Park, T.H. Park, J.J. Lee, J. Joo, J. Vac. Sci. Technol. A 18 (2000) 524.
[27] P. Hones, C. Zakri, P.E. Shmid, F. Lery, O.R. Shojel, Appl. Phys. Lett. 76 (2000) 3194.
[28] D.S. Rickerby, S.J. Bull, in: D. Dowson, et al. (Eds.), Proceedings of the 16th Leeds-Lyon Symposium on Tribology: 'Mechanics of Coatings', Elsevier, Amsterdam, 1990, p. 337.
[29] J.A. Thornton, J. Vac. Sci. Technol. A 4 (1986) 2309.
[30] S.J. Bull, D.S. Rickerby, T. Robertson, A. Hendry, Surf. Coat. Technol. 36 (1988) 743.
[31] W.C. Oliver, G.M. Phar, J. Mater. Res. 7 (1992) 1564.